Published in final edited form as:
Neurotoxicology. 2007 May ; 28(3): 478–489.

Gene Expression Profiling of Human Primary Astrocytes Exposed to Manganese Chloride Indicates Selective Effects on Several Functions of the Cells

Amitabha Sengupta[1,#], **Sarah M. Mense**[1,#], **Changgui Lan**[1], **Mei Zhou**[1], **Rory E. Mauro**[1], **Lisa Kellerman**[1], **Galina Bentsman**[2], **David J. Volsky**[2], **Elan D. Louis**[3], **Joseph H. Graziano**[1], and **Li Zhang**[1,*]

1*Department of Environmental Health Sciences, Columbia University, Mailman School of Public Health, 60 Haven Avenue, B-106, New York, New York 10032*

2*Molecular Virology Division, St. Luke's-Roosevelt Hospital Center and College of Physicians and Surgeons, Columbia University, New York, New York 10019*

3*Gertrude H. Sergievsky Center and the Department of Neurology, Columbia University, New York 10032*

Abstract

Exposure of adult humans to manganese (Mn) has long been known to cause neurotoxicity. Recent evidence also suggests that exposure of children to Mn is associated with developmental neurotoxicity. Astrocytes are critical for the proper functioning of the nervous system, and they play active roles in neurogenesis, synaptogenesis and synaptic neurotransmission. In this report, to help elucidate the molecular events underlying Mn neurotoxicity, we systematically identified the molecular targets of Mn in primary human astrocytes at a genome-wide level, by using microarray gene expression profiling and computational data analysis algorithms. We found that Mn altered the expression of diverse genes ranging from those encoding cytokines and transporters to signal transducers and transcriptional regulators. Particularly, 28 genes encoding proinflammatory chemokines, cytokines and related functions were up-regulated whereas 15 genes encoding functions involved in DNA replication and repair and cell cycle checkpoint control were down-regulated. Consistent with the increased expression of proinflammatory factors, analysis of common regulators revealed that 16 targets known to be positively affected by the interferon-γ signaling pathway were up-regulated by Mn^{2+}. In addition, 68 genes were found to be similarly up- or down-regulated by both Mn^{2+} and hypoxia. These results from genomic analysis are further supported by data from real-time RT-PCR, Western blotting, flow cytometric and toxicological analyses. Together, these analyses show that Mn^{2+} selectively affects cell cycle progression, the expression of hypoxia-responsive genes, and the expression of proinflammatory factors in primary human astrocytes. These results provide important insights into the molecular mechanisms underlying Mn neurotoxicity.

Keywords

Manganese; Inflammatory factors; Human Astrocytes; Microarray; Gene expression

*Corresponding Author: Email: lz2115@columbia.edu Tel: 212-781-1038, Fax: 212-781-1038
#Contributed to this work equally

Introduction

Manganese (Mn) is an essential metal required for many enzymatic reactions such as those catalyzed by arginase, glutamine synthetase and manganese-dependent superoxide dismutase. However, elevated Mn exposures can lead to its accumulation in the brain and causes serious neurotoxicity (Crossgrove and Zheng, 2004;Dobson et al., 2004;Erikson et al., 2004a;Hazell, 2002;Newland, 1999;Pal et al., 1999). In humans, Mn deficiency is rare whereas Mn neurotoxicity or manganism can occur due to occupational and environmental exposures (Crossgrove and Zheng, 2004;Pal et al., 1999). It is estimated that over 3700 tons of Mn are released into the atmosphere every year (2001), particularly from the gasoline additive, methylcyclopentadienyl manganese tricarbonyl (MMT). Signs of manganism resemble those of idiopathic Parkinson's disease, including dystonia, bradykinesia, rigidity, and tremor (Barbeau, 1984;Newland, 1999;Pal et al., 1999). In exposed humans and monkeys, Mn accumulates at the highest levels in the striatum, globus pallidus, and substantia nigra (Erikson et al., 2004a). In monkeys dosed for three months with MnO_2, Mn concentrations reached 264 μM in the striatum and 334 μM in the globus pallidus (Suzuki et al., 1975). Mn exposure may also cause developmental neurotoxicity in children. A recent cross-sectional study of 201 ten year-old children living in Araihazar, Bangladesh showed that water Mn was significantly and adversely associated with Performance and Full Scale raw intelligence score (Wasserman et al., 2005).

Previous studies have suggested that Mn^{2+} can induce oxidative stress and affect iron metabolism and cellular energy metabolism (Dobson et al., 2004;Erikson et al., 2004a;Hazell, 2002;Li et al., 2005;Lu et al., 2005). Nonetheless, the understanding of the specific mechanisms underlying Mn neurotoxicity in humans remains far from clear. In mammals, Mn is absorbed and transported to the brain by the mechanisms responsible for the uptake of divalent metal ions, including the DMT-1-mediated and transferrin-mediated pathways (Erikson and Aschner, 2006;Erikson et al., 2004b). In the brain, astrocytes are a “sink” for Mn, with concentrations 10-50-fold higher than in neurons (Erikson and Aschner, 2006;Erikson et al., 2004b). Mn transport to astrocytes is significantly affected by Fe status. Also, evidence suggests that Mn transport involves multiple pathways that may be competitive or synergistic with iron transport (Crossgrove and Yokel, 2005;Erikson and Aschner, 2006;Erikson et al., 2004b).

In this report, we focus on the potential effects of Mn on human astrocytes. Astrocytes play active roles in many neuronal functions: maintaining ion and pH homeostasis, promoting the synthesis and removal of neurotransmitters, providing glucose supply and antioxidant defense, and regulating synaptic activity, synaptogenesis and neurogenesis (Auld and Robitaille, 2003;Magistretti and Ransom, 2002;Newman, 2003). Astrocytes are sensors of the brain environment, to which they immediately react on the genomic (gene expression) and non-genomic levels (Nedergaard and Dirnagl, 2005). Inflammatory activation of astrocytes or astrocyte dysfunctions are believed to be associated with several chronic neurological diseases, including prion, Alzheimer's and Parkinson's Diseases, and HIV-1 associated dementia (HAD) (Burwinkel et al., 2004;Choi et al., 2005;Meda et al., 2001;Wang et al., 2004). If Mn neurotoxicity is linked with inflammation, it is plausible that the initiating events may occur in astrocytes. One purpose of this study is to test the hypothesis that Mn may induce the expression of inflammatory mediators in astrocytes.

A new powerful way to begin identifying molecular targets of pathogenic insults to cells is to use microarray technology to obtain a general gene expression profile of affected versus control cells. Candidate affected genes and their functions can then be subjected to in-depth analysis to determine the mechanisms of their responses to a given stimulus. Here we applied this approach to identify candidate genes and gene families in human primary astrocytes that are affected by exposure of the cells to Mn^{2+}. Furthermore, we applied biochemical and

toxicological methods to confirm the prominent effects of Mn^{2+} in primary human astrocytes. Our studies suggest that Mn^{2+} selectively affects cell cycle progression and the expression of hypoxia-responsive genes and proinflammatory factors. These results provide new insights into the mechanisms underlying Mn neurotoxicity.

Materials and Methods

Primary human astrocytes and treatment

Astrocytes were isolated from second trimester (14–19 weeks of gestational age) human fetal brains obtained from elective abortions in full compliance with NIH guidelines, as previously described by Dr. Volsky and colleagues (Canki et al., 2001;Wang et al., 2004). Homogenous preparations of astrocytes were obtained using high-density culture conditions in the absence of growth factors in F12 Dulbecco's modified Eagles Medium (DMEM-F12) (GIBCO-Invitrogen, Carlsbad, CA) containing 10% fetal bovine serum (FBS), penicillin, streptomycin, and gentamycin. Cells were maintained in this medium at $2–5 \times 10^4$ cells/cm^2 and subcultured weekly up to six times. Cultures were regularly monitored by immunofluorescence staining for expression of the astrocytic marker glial fibrillary acidic protein (GFAP) and HAM-56 to identify cells of the monocyte lineage. Only cultures that contained ≥99% GFAP-positive astrocytes and no detectable HAM-56-positive cells were used in the experiments. Primary human astrocytes were treated with or without 200 μM $MnCl_2$.

Cell growth and LDH assays

To measure the effect of $MnCl_2$ on the growth rate of primary human astrocytes, 1.2×10^4 cells were plated on each well of 24-well plates. Cells were treated with the desired concentrations of $MnCl_2$ for 7 days. Then, adherent, live cells were collected by trypsin treatment, and the number of cells was accounted by using a hemacytometer. At least three independent sets of data were collected in each experiment. To assess the effect of $MnCl_2$ on cell viability of astrocytes, we measured the release of lactate dehydrogenase (LDH) into the medium. In this case, 7.5×10^4 cells were plated on each well of 24-well plates and treated with the desired concentrations of $MnCl_2$ for 7 days. The medium was collected, and lactate dehydrogenase (LDH) activities were measured and calculated by using a kit purchased from Sigma (Saint Louis). The total cellular LDH activity was measured by detecting the activity in Triton X-100 lysed cells (Ehrich and Sharova, 2000).

RNA extraction and Affymetrix GeneChip expression analysis

Primary human astrocytes (passage 4) were treated with or without 200 μM $MnCl_2$ for 7 days. Total RNA was extracted by using TRIzol reagent (GIBCOBRL Life Technologies). The quality of RNA was high as assessed by measuring absorbance at 260 and 280 nm, by gel electrophoresis, and by the quality of microarray data (see below). We isolated RNA from three independent batches of human astrocytes, which were from different subjects. No identifiable information from these subjects was available, in keeping with the guidelines on human subjects. Three independent batches of astrocytes from three different subjects, not the same subject, were used to ensure that our data and conclusions would not totally rely on one unidentified subject, who may have experienced influential environmental or genetic conditions. The synthesis of cDNAs and biotin-labeled cRNAs were carried out exactly as described in the Affymetrix GeneChip Expression Analysis Technical Manual (2000). The human genome U133 plus 2.0 arrays were purchased from Affymetrix, Inc. Probe hybridization and data collection were carried out by the Columbia University Affymetrix GeneChip processing center. Initial data analysis was performed by using the Affymetrix Microarray suite.

Computational analysis of microarray data

We analyzed microarray expression data by applying a series of quality control, statistical, filtering, gene ontology, and pathway analysis algorithms. First, by using GCOS1.2 with the advanced PLIER (probe logarithmic intensity error) algorithm, we calculated and examined the parameters reflecting the image quality of the arrays. Arrays with a high background level in any region were discarded and replaced. The average noise or background level was limited to less than 5%. The average intensity for those genes judged to be present was at least 10-fold higher than those judged to be absent. Also, arrays that deviated considerably in the percentage of present and absent genes from the majority of the arrays were replaced. Arrays with a β-actin 3′/5′ ratio greater than 2 were replaced. Next, microarray data were uploaded to GeneSpring 7.0 (Silicon Genetics) for further quality and statistical analysis. The data were normalized again by using the stringent per chip and per gene normalization algorithms; genes with low control signal (less than average) or not present in 1/3 of the samples were dropped out, before statistical analysis. The data were then analyzed by nonparametric two-way ANOVA (one parameter is cell, another parameter is treatment). The Benjamini & Hochberg false discovery rate multiple testing correction was applied with a false discovery rate of less than 5%. Two-way ANOVA was chosen for statistical analysis because the variations of astrocytes from different subject can be significant, and in certain cases, may exert stronger effects than the treatment of cells. Two-way ANOVA would take account of this and identify statistically significant genes whose transcript level was consistently altered by Mn. Second, to identify genes whose transcript level was significantly altered by Mn, we applied four consecutive filtering processes: The first three were applied to identify genes whose transcript level was altered by at least 1.5-fold (Mn-treated vs control) in every batch of human astrocytes. The last one was applied to identify genes whose overall transcript level calculated from three independent batches of astrocytes was altered by at least 2-fold. The folds of changes listed in the Tables are the overall changes calculated from data from the three batches of astrocytes by GeneSpring, which combines data from all three controls and three Mn^{2+}-treated samples.

The identified Mn^{2+}-altered genes were further analyzed and categorized by using various biological annotation programs including the DAVID/EASE program provided by NIAID (http://apps1.niaid.nih.gov/david/upload.asp) and the Gene Ontology (GO) algorithm in GeneSpring. Data from OMIM and the literature were also used to categorize the genes. Our analyses led to the identification of six notable functional groups of genes whose expression is altered by Mn^{2+} (see Results). Finally, we used another computational program called PathwayAssist (Stratagene Software) to analyze Mn^{2+}-altered genes. This program uses information available in the current literature to identify common pathways, targets or regulators that are associated with the altered genes.

Quantitative real-time reverse-transcription-polymerase chain reaction (real-time RT-PCR)

Oligonucleotide primers for measuring transcript levels of genes were designed based on the sequences used to design microarray probes by using the primer 3 program (http://frodo.wi.mit.edu/cgi-bin/primer3/primer3_www.cgi). β-actin was used as a control for the relative quantification of transcripts, because our microarray data showed that the β-actin transcript level was unaffected by Mn^{2+}. RT-PCR reactions were performed by using a Roche LightCycler and the SYBR green kit according to specified protocols. Calculations were done by using the Roche LightCycler software (Bustin, 2002;Giulietti et al., 2001;Livak and Schmittgen, 2001). Primer sequences used for real-time PCR are listed in supplemental Table S1.

Flow cytometric analysis

Primary human astrocytes, seeded at 2×10^5 cells/cm^2, were treated with no reagent (control) or 200 μM $MnCl_2$ (Mn-treated) for 7 days. Then cells were collected by trypsinization and

prepared for FACS analysis, as described (Darzynkiewicz et al., 1999). Briefly, cells were fixed in 70% ethanol and then stained with propidium iodide. 10^6 to 10^7 cells were used for each FACS analysis at the Columbia University Medical Center FACS analysis facility. Flow cytometric analysis was performed by using a Becton-Dickinson FACSCalibur instrument. Data were acquired by using the CellQuest PRO (Becton-Dickinson) software, and were analyzed by combining CellQuest PRO and FloJo (TreeStar) software.

Western blotting analysis

Astrocytes were washed twice in PBS, and whole-cell extracts were prepared by adding 10 packed cell volumes of 1x sample buffer (2% SDS, 100 mM dithiothreitol, 60 mM Tris pH 6.8, and 10% glycerol) and boiled for 5 minutes. Protein concentrations were determined by using the bicinchoninic acid (BCA) protein assay kit (Pierce). Approximately 20 μg protein was analyzed on 9% SDS-PAGE and transferred onto the Immuno-Blot PVDF Membrane (Bio-Rad). The membranes were probed with polyclonal antibodies, followed by detection with a chemiluminescence Western blotting kit (Boehringer Mannheim). Polyclonal antibodies against SOD2, COX2 and β-actin were purchased from Santa Cruz Biotechnology, Inc., Abcam Inc. and Cell Signaling Technology, respectively. The primary antibodies were used at 1:1000 dilution, while the secondary antibody was used at 1:2500 dilution.

Results

Mn^{2+} alters the transcript levels of a subset of genes with distinctive functional characteristics

Previous studies of Mn-exposed monkeys and rats showed that Mn concentration in the striatum and globus pallidus can reach concentrations higher than 200 μM (Erikson et al., 2004a;Suzuki et al., 1975). In addition, Mn concentration in astrocytes can be much higher than in neurons. Thus, to maximize the likelihood of identifying Mn targets that may be relevant to human exposures, we chose to examine the effect of 200 μM Mn on primary human astrocytes. We performed microarray gene expression analysis by using RNA samples from three independent batches of primary human astrocytes, treated with or without $MnCl_2$ for 7 days. We used a series of quality control, normalization, statistical and filtering analysis algorithms to identify the differentially expressed genes in Mn^{2+}-treated vs. untreated astrocytes, see Materials and Methods. We identified genes whose overall expression level in three independent batches of astrocytes was altered by > 2-fold and whose expression level in each batch of astrocytes was altered by >1.5-fold. We used these stringent statistical criteria to minimize the identification of false positive targets.

We identified 734 genes whose expression was selectively altered by Mn^{2+} (Table 1). 414 were up-regulated while 320 were down-regulated. Among them, about 316 are annotated to date (Table 1). The transcript levels of these altered genes in three different batches of astrocytes were displayed in Figure 1A (up-regulated) and 1B (down-regulated). By using the NIH program DAVID, PubMed, and the gene ontology algorithm GeneSpring, we identified several functionally distinctive classes of genes altered by Mn^{2+}. These identified categories included genes encoding cytokines and inflammatory functions, regulators of cell cycle, DNA replication and repair, transporters, functions involved in development, transcriptional regulators and signal transducers (Table 1).

To confirm the results form microarray gene expression profiling, we used real-time RT-PCR analysis. We selectively examined the transcript levels of a series of Mn^{2+}-altered genes, particularly those encoding inflammatory mediators, such as CD48, CR1, CXCL2, CD8B1, CXC3, and IL12A. Figure 2A shows that consistent with microarray data, Mn^{2+} significantly

induced the expression of CD48, SOD2, CR1, CXCL2, CD8B1, IL12A, CNOT6L, GAL, HEPH (hephaestin), MYT1L, POU1F1, SULT1C1, and CXCL3.

In addition, we performed dose-response analysis of SOD2 and CXCL2 transcript levels (Figure 2B and C). We found that 200 μM Mn^{2+} dramatically increased their transcript levels, whereas 10 μM and 50 μM Mn^{2+} did not (Figure 2B and 2C). This dose-response pattern is further confirmed by Western blotting analysis. As shown in Figure 3, 200 μM Mn^{2+} significantly increased SOD2 (Figure 3A) and COX2 (Figure 3B) protein levels (Figure 3), although 10 or 50 μM did not, after 7 days of treatment. Still, this effect of Mn^{2+} is likely relevant to human exposures, because Mn^{2+} concentration can reach higher than 200 μM in the brain and because Mn^{2+} can be elevated further in astrocytes (Erikson and Aschner, 2006;Fitsanakis et al., 2006;Suzuki et al., 1975). These results from real-time RT-PCR and Western blotting analyses support the validity of our microarray gene expression analysis.

A group of genes encoding functions involved in cell cycle control and DNA replication and repair was selectively down-regulated

We found that 15 genes encoding functions involved in DNA replication and repair and cell cycle checkpoint control were down-regulated (Tables 1 and 2). Among these, of particular interest are ATM kinase (ataxia telangiectasia mutated), the checkpoint kinase BUB1, the Fanconi anemia FANCF protein, two subunits of DNA primase PRIM1 and PRIM2A, and the replication factor RFC5 (Abraham and Tibbetts, 2005;Margolis, 2004). Remarkably, by using flow cytometric analysis, we found that Mn^{2+} caused the accumulation of astrocytes in the S phase of the cell cycle (Table 3). This effect on cell cycle is entirely consistent with the effect of Mn^{2+} on the expression of genes involved in DNA replication and repair, as described above. Very likely, cells accumulated in the S phase cannot progress further and stop growing. Indeed, we found that the growth rate of Mn^{2+}-treated astrocytes was significantly reduced (Figure 4A). However, no apoptotic cells were detected by TUNEL assays, even after prolonged incubation with 200 μM Mn^{2+} for 2 weeks (not shown). The lack of cell death is also supported by the measurement of LDH release to the medium. As shown in Figure 4B, LDH release to the medium in cells treated with 200 μM Mn^{2+} was barely increased by 2% (from 6.6% in untreated cells to 8.8%). This increase is only of marginal statistic significance, with a p-value of 0.06 (Figure 4B).

A group of genes encoding cytokines and immune functions was selectively up-regulated in Mn^{2+}-treated human astrocytes

Mn^{2+} appears to induce the transcript levels of a group of genes that encode cytokines, chemokines and other immune functions in primary human astrocytes (Tables 1 and 4). Specifically, Mn^{2+} up-regulated a series of proinflammatory cytokines and chemokines, including CCL7 (MCP3), CXCL14, CXCL2 (MIP2A), CXCL3 (MIP2B), CXCL6 (GCP2), defensin DEFB103, epiregulin EREG, and interleukins IL12A and IL7 (Tables 1 and 4). Other up-regulated pro-inflammatory or immune functions include CD40 and CD8 antigen, the DR subunit of the class II major histocompatibility complex HLA-DRB4, cyclooxygenase COX2 (PTGS2), and pentaxin-related gene PTX3 (Parslow et al., 2001). Notably, the transcript levels of several angiogenic growth factors, including adrenomedullin (ADM), angiopoietin-like 4 (ANGPTL4), placental growth factor (PGF), and vascular endothelial growth factor (VEGF), were up-regulated (Tables 4 and 5). These factors are also induced by hypoxia in various cells (Iimuro et al., 2004;Manalo et al., 2005;Tait and Jones, 2004). In another study, we identified hypoxia-responsive genes in human astrocytes (Mense et al., 2006). Comparison of hypoxia-responsive genes with Mn^{2+}-responsive genes identified 68 genes that were affected by hypoxia and Mn^{2+} in the same manner (Table 5). Fifty genes were up-regulated, and 18 genes were down-regulated by both Mn^{2+} and hypoxia in primary human astrocytes (Table 5).

Mn^{2+} caused changes in the transcript levels of a number of transporters

Our gene ontology analyses identified 18 genes encoding functions involved in the transport of proteins, small molecules and ions that were up-regulated while an equal number of genes were down-regulated (Table 1 and Supplemental Table S2). These transporters include ABC transporters (up-regulated, ABCA9; and down-regulated, ABCA5); cholesterol transporters APOL1 and APOL2; transporters of small molecules and ions, including SLC11A2 (DMT1), SLC16A3, SLC2A13, SLC22A15, SLC4A10; functions involved in Ca^{2+} entry, including the channel proteins TRPM1 and TRPM4, and the inhibitor of Ca^{2+} channel phospholamban PLN; functions involved in membrane and vesicle trafficking RAB21, RAB23, SEC15L1 and VPS13A; and the nuclear import receptor importin IPO11 (Harteneck, 2005;Plafker and Macara, 2000). Interestingly, a recent microarray analysis of gene expression in the prefrontal cortex of schizophrenia and control brains revealed the significant up-regulation of the APOL1 and APOL2 genes (Mimmack et al., 2002).

Mn^{2+} altered the transcript levels of a number of genes encoding developmentally relevant functions

Our analyses identified 38 (up-regulated, 25; down-regulated, 13) additional Mn^{2+}-altered genes (besides those relevant ones shown in Tables 2, 4 and S2) encoding developmentally-relevant functions (Tables 1 and supplemental Table S3). Among the up-regulated 25 genes (supplemental Table S3), CELSR1, neuregulin NRG2, neuropilin NRP1, calcyclin S100A6 and transcriptional regulators POU1F1, NOTCH4, FOXP2 and TFAP2B (Mani et al., 2005) are known to play important roles in mammalian neural development or are expressed in neural cells. Notably, neuregulin NRG2 (Michailov et al., 2004) (Table S3), a member of the ERBB family of tyrosine kinase transmembrane receptors including the EGF receptor, and epiregulin (Park et al., 2004), a member of the epidermal growth factor family (Table 4), were both up-regulated. Likewise, neuropilin NRP1 (Castellani, 2002), a receptor for VEGF (Table S3), and VEGF (Table 4), were both up-regulated. Evidently, both the EGF and VEGF signaling pathways may be affected by Mn^{2+} in astrocytes.

The transcript levels of a number of signal transducers and transcriptional regulators were altered by Mn^{2+}

The effects of Mn^{2+} on gene expression (Table 1) are presumably mediated by their effects (direct or indirect) on the levels or activities of transcriptional regulators and/or their upstream effectors, i.e., signal transducers. Thus, it is expected that the expression of certain transcriptional regulators and signal transducers would be altered by Mn^{2+}. Indeed, our analyses identified a series of signal transducers and transcriptional regulators whose transcript level was altered by Mn^{2+}. In total, we identified about 41 altered signal transducers and 30 altered transcriptional regulators (Table 1). Tables S4 and S5 list those additional 21 altered signal transducers and 19 altered transcriptional regulators, besides those already shown in Tables 2, 4, S2, and S3, such as IGB5, FOXP2 and POU1F1. The alteration of the transcript levels of some of these signal transducers and transcriptional regulators would likely contribute to the alteration of downstream genes shown in Tables 2, 4, S2, and S3, although too little is known to correlate these regulators with their downstream effects in most cases. Interestingly, the hypoxia-inducible factor HIF1A was up-regulated whereas its inhibitor HIF1AN (Mahon et al., 2001) was down-regulated. This opposing effect of Mn^{2+} on HIF1A and HIF1AN expression is in complete agreement with their perspective functions and with the result that 68 genes, such as ADM and VEGF (Table 5), that were induced/suppressed by Mn^{2+} were also induced/suppressed by hypoxia (Mense et al., 2006).

The IFN-γ and EGF signaling pathways might be perturbed by Mn^{2+} in primary human astrocytes

To identify common signaling pathways that may mediate the effects of Mn^{2+} on gene expression, we used a computational program called PathwayAssist (Stratagene Software). We found that Mn^{2+} altered the transcript levels of genes that are targets of the IFN-γ signaling pathway (Schroder et al., 2004) and the EGF signaling pathway (Schlessinger, 2004). Twenty-six altered genes are known to be the targets of the IFN-γ signaling pathway while 11 are known to be the targets of the EGF signaling pathway (Table 6). Particularly, among those targets of the IFN-γ signaling pathway, 20 of them were shown to be positively affected by the IFN-γ signaling pathway in certain human cells, and 16 out of 20 were also up-regulated by Mn^{2+} (see italicized genes in Table 6).

Discussion

In this report, we applied microarray gene expression profiling and computational algorithms to identify molecular targets of the common environmental toxicant Mn^{2+} in primary human astrocytes. Further, we used real-time RT-PCR, Western blotting, flow cytometric, and toxicological analyses to confirm the key results from microarray expression analysis. Our analyses provide several new insights into the molecular neurotoxic actions of Mn. Such insights may provide a molecular basis for further studies to elucidate the molecular events underlying Mn neurotoxicity in humans. First, data from microarray expression profiling (Table 2), flow cytometry (Table 3), and measurement of cell growth and LDH release (Figure 4) show that Mn^{2+} selectively affected astrocyte cell proliferation, while it did not significantly affect cell death.

Second, 68 induced/suppressed genes by Mn^{2+}, such as angiogenic factors (e.g., ADM, ANGPTL4 and VEGF) and SOD2 (Table 5), were also induced/suppressed by hypoxia. Consistent with this, we found that 11 target genes of the EGF signaling pathway were also targeted by Mn^{2+} (Table 6). In a previous analysis (Mense et al., 2006), we found that hypoxia induced nearly 40 genes that are targets of the EGF signaling pathway. These results raise the possibility that Mn treatment and hypoxia act on a significant number of common target genes and that Mn treatment resembles certain aspects of brain hypoxia or ischemia.

Third, a series of genes encoding proinflammatory functions was up-regulated by Mn^{2+} (Table 4). Particularly, the transcript levels of several genes encoding proinflammatory chemokines, CCL7 (MCP3), CXCL14, CXCL2 (MIP2A), CXCL3 (MIP2B) and CXCL6 (GCP2), and interleukins IL12A and IL7, were all enhanced in Mn^{2+}-treated astrocytes. Proinflammatory chemokines and cytokines are thought to play a critical role in the induction and perpetuation of inflammation in the brain (Burwinkel et al., 2004;Choi et al., 2005;Meda et al., 2001). Furthermore, 16 known targets of the IFN-γ signaling pathway that are activated by the pathway were also activated (Table 6), suggesting the IFN-γ signaling pathway was activated in Mn^{2+}-treated astrocytes although the transcript level of IFN-γ per se was not detected to be increased. IFN-γ plays a major immunomodulatory role in astrocytes, and the activation of its signaling pathway leads to the expression of various inflammation-associated molecules (Choi et al., 2005;Lin et al., 2004), as those shown in Tables 4 and 6. Glial activation and the production of proinflammatory chemokines and cytokines have been shown to be associated with many central nervous system (CNS) diseases, such as bacterial or viral infection, multiple sclerosis, prion infection, Parkinson's disease, Alzheimer's disease and ischemia (Burwinkel et al., 2004;Choi et al., 2005;Meda et al., 2001).This association is in complete agreement with our findings that proinflammatory chemokines and cytokines are up-regulated and that the IFN-γ signaling pathway may be activated by Mn^{2+} in astrocytes.

Interestingly, several genes shown in Tables S4 and S5 are known to be expressed in the brain and/or to play important roles in the proper CNS functioning. These include the GABA A receptor GABRG2, galanin (GAL), the G protein-coupled receptor GPR24, protocadherins PCDH7 and PCDHA6, RGS2, catenins CTNNA1 and CTNNB1, poliovirus receptor PVR, the neurokinin 1 receptor TACR1, presenilin binding protein CSEN, and myelin transcription factor 1-like MYT1L. Particularly, galanin is a 29 amino acid neuropeptide that plays many important roles in CNS (Robinson, 2004). It can modulate gastrointestinal motility, pituitary hormone release, neurotrophic action, nociception, anxiety, feeding and cognition (Robinson, 2004;Wrenn et al., 2004). GPR24 (MCHR1) may be involved in the control of obesity, depression and/or anxiety (Georgescu et al., 2005). CSEN appears to play important roles in pain processing (Cheng et al., 2002) while MYT1L is expressed in neural cells of the developing mammalian CNS (Kim et al., 1997).

In summary, our studies using a combination of genomic, biochemical and toxicological approaches uncovered several note-worthy characteristics of the effects of Mn^{2+} on primary human astrocytes. The most striking characteristics include its effects on cell cycle progression, the expression of hypoxia-responsive genes and the expression of proinflammatory factors. The effects of Mn^{2+} on the expression of hypoxia-responsive genes and proinflammatory factors are consistent with the previous finding that the production of proinflammatory cytokines is increased in mouse astrocytes following ischemia (Lau and Yu, 2001). Our findings provide a molecular basis for further investigation of the mechanisms underlying Mn neurotoxicity and perhaps even other neurodegenerative diseases. With a better understanding of the functions of signal transducers and transcriptional regulators and mechanisms of gene regulation, our data may provide further insights into the molecular events underlying Mn neurotoxicity.

Supplementary Material

Refer to Web version on PubMed Central for supplementary material.

Acknowledgements

This work is supported in part by public health grants HL65568 (LZ) and NS31492 (GB and DJV).

References

International Manganese Institute brochure. In International Manganese Institute (Paris, France), 2001.

Abraham RT, Tibbetts RS. Cell biology. Guiding ATM to broken DNA. Science 2005;308:510–511. [PubMed: 15845843]

Auld DS, Robitaille R. Glial cells and neurotransmission: an inclusive view of synaptic function. Neuron 2003;40:389–400. [PubMed: 14556716]

Barbeau A. Manganese and extrapyramidal disorders (a critical review and tribute to Dr. George C. Cotzias). Neurotoxicology 1984;5:13–35. [PubMed: 6538948]

Burwinkel M, Riemer C, Schwarz A, Schultz J, Neidhold S, Bamme T, Baier M. Role of cytokines and chemokines in prion infections of the central nervous system. Int J Dev Neurosci 2004;22:497–505. [PubMed: 15465279]

Bustin SA. Quantification of mRNA using real-time reverse transcription PCR (RT-PCR): trends and problems. J Mol Endocrinol 2002;29:23–39. [PubMed: 12200227]

Canki M, Thai JN, Chao W, Ghorpade A, Potash MJ, Volsky DJ. Highly productive infection with pseudotyped human immunodeficiency virus type 1 (HIV-1) indicates no intracellular restrictions to HIV-1 replication in primary human astrocytes. J Virol 2001;75:7925–7933. [PubMed: 11483737]

Castellani V. The function of neuropilin/L1 complex. Adv Exp Med Biol 2002;515:91–102. [PubMed: 12613546]

Cheng HY, Pitcher GM, Laviolette SR, Whishaw IQ, Tong KI, Kockeritz LK, Wada T, Joza NA, Crackower M, Goncalves J, et al. DREAM is a critical transcriptional repressor for pain modulation. Cell 2002;108:31–43. [PubMed: 11792319]

Choi WH, Ji KA, Jeon SB, Yang MS, Kim H, Min KJ, Shong M, Jou I, Joe EH. Anti-inflammatory roles of retinoic acid in rat brain astrocytes: Suppression of interferon-gamma-induced JAK/STAT phosphorylation. Biochem Biophys Res Commun 2005;329:125–131. [PubMed: 15721283]

Crossgrove J, Zheng W. Manganese toxicity upon overexposure. NMR Biomed 2004;17:544–553. [PubMed: 15617053]

Crossgrove JS, Yokel RA. Manganese distribution across the blood-brain barrier. IV. Evidence for brain influx through store-operated calcium channels. Neurotoxicology 2005;26:297–307. [PubMed: 15935202]

Darzynkiewicz, Z.; Juan, G.; Bedner, E. Determining cell cyle stages by flow cytometry. In: Bonifacino, JS.; Dasso, M.; Harford, JB.; Lippincott-Schwartz, J.; Yamada, KM., editors. Current protocols in cell biology. New York: John Wiley & Sons, Inc.; 1999. p. 8.4.1-8.4.18.

Dobson AW, Erikson KM, Aschner M. Manganese neurotoxicity. Ann N Y Acad Sci 2004;1012:115–128. [PubMed: 15105259]

Ehrich, M.; Sharova, L. In vitro methods for detecting cytotoxicity. In: Maines, MD.; Costa, LTG.; Reed, DJ.; Sassa, S.; Sipes, IG., editors. Current protocols in toxicology. New York: John Wiley & Sons, Inc; 2000. p. 2.6.1-2.6.27.

Erikson KM, Aschner M. Increased manganese uptake by primary astrocyte cultures with altered iron status is mediated primarily by divalent metal transporter. Neurotoxicology 2006;27:125–130. [PubMed: 16140386]

Erikson KM, Dobson AW, Dorman DC, Aschner M. Manganese exposure and induced oxidative stress in the rat brain. Sci Total Environ 2004a;334-335:409–416. [PubMed: 15504526]

Erikson KM, Syversen T, Steinnes E, Aschner M. Globus pallidus: a target brain region for divalent metal accumulation associated with dietary iron deficiency. J Nutr Biochem 2004b;15:335–341. [PubMed: 15157939]

Fitsanakis VA, Zhang N, Avison MJ, Gore JC, Aschner JL, Aschner M. The use of magnetic resonance imaging (MRI) in the study of manganese neurotoxicity. Neurotoxicology 2006;27:798–806. [PubMed: 16620989]

Georgescu D, Sears RM, Hommel JD, Barrot M, Bolanos CA, Marsh DJ, Bednarek MA, Bibb JA, Maratos-Flier E, Nestler EJ, DiLeone RJ. The hypothalamic neuropeptide melanin-concentrating hormone acts in the nucleus accumbens to modulate feeding behavior and forced-swim performance. J Neurosci 2005;25:2933–2940. [PubMed: 15772353]

Giulietti A, Overbergh L, Valckx D, Decallonne B, Bouillon R, Mathieu C. An overview of real-time quantitative PCR: applications to quantify cytokine gene expression. Methods 2001;25:386–401. [PubMed: 11846608]

Harteneck C. Function and pharmacology of TRPM cation channels. Naunyn Schmiedebergs Arch Pharmacol. 2005

Hazell AS. Astrocytes and manganese neurotoxicity. Neurochem Int 2002;41:271–277. [PubMed: 12106778]

Iimuro S, Shindo T, Moriyama N, Amaki T, Niu P, Takeda N, Iwata H, Zhang Y, Ebihara A, Nagai R. Angiogenic effects of adrenomedullin in ischemia and tumor growth. Circ Res 2004;95:415–423. [PubMed: 15242974]

Kim JG, Armstrong RC, v Agoston D, Robinsky A, Wiese C, Nagle J, Hudson LD. Myelin transcription factor 1 (Myt1) of the oligodendrocyte lineage, along with a closely related CCHC zinc finger, is expressed in developing neurons in the mammalian central nervous system. J Neurosci Res 1997;50:272–290. [PubMed: 9373037]

Lau LT, Yu AC. Astrocytes produce and release interleukin-1, interleukin-6, tumor necrosis factor alpha and interferon-gamma following traumatic and metabolic injury. J Neurotrauma 2001;18:351–359. [PubMed: 11284554]

Li GJ, Zhao Q, Zheng W. Alteration at translational but not transcriptional level of transferrin receptor expression following manganese exposure at the blood-CSF barrier in vitro. Toxicol Appl Pharmacol 2005;205:188–200. [PubMed: 15893546]

Lin W, Kemper A, McCarthy KD, Pytel P, Wang JP, Campbell IL, Utset MF, Popko B. Interferon-gamma induced medulloblastoma in the developing cerebellum. J Neurosci 2004;24:10074–10083. [PubMed: 15537876]

Livak KJ, Schmittgen TD. Analysis of relative gene expression data using real-time quantitative PCR and the 2(-Delta Delta C(T)) Method. Methods 2001;25:402–408. [PubMed: 11846609]

Lu L, Zhang LL, Li GJ, Guo W, Liang W, Zheng W. Alteration of serum concentrations of manganese, iron, ferritin, and transferrin receptor following exposure to welding fumes among career welders. Neurotoxicology 2005;26:257–265. [PubMed: 15713346]

Magisretti, PJ.; Ransom, BR. Astrocytes. In: Davis, KL.; Charney, D.; Coyle, JT.; Nemeroff, C., editors. Neuropsychopharmacology: The Fifth Generation of Progress. American College of Neuropsychopharmacology; 2002. (online)

Mahon PC, Hirota K, Semenza GL. FIH-1: a novel protein that interacts with HIF-1alpha and VHL to mediate repression of HIF-1 transcriptional activity. Genes Dev 2001;15:2675–2686. [PubMed: 11641274]

Manalo DJ, Rowan A, Lavoie T, Natarajan L, Kelly BD, Ye SQ, Garcia JG, Semenza GL. Transcriptional regulation of vascular endothelial cell responses to hypoxia by HIF-1. Blood 2005;105:659–669. [PubMed: 15374877]

Mani A, Radhakrishnan J, Farhi A, Carew KS, Warnes CA, Nelson-Williams C, Day RW, Pober B, State MW, Lifton RP. Syndromic patent ductus arteriosus: evidence for haploinsufficient TFAP2B mutations and identification of a linked sleep disorder. Proc Natl Acad Sci U S A 2005;102:2975–2979. [PubMed: 15684060]

Margolis RL. Bub1, a gatekeeper for Cdc20-dependent mitotic exit. Dev Cell 2004;7:634–635. [PubMed: 15525525]

Meda L, Baron P, Scarlato G. Glial activation in Alzheimer's disease: the role of Abeta and its associated proteins. Neurobiol Aging 2001;22:885–893. [PubMed: 11754995]

Mense SM, Sengupta A, Zhou M, Lan C, Bentsman G, Volsky DJ, Zhang L. Gene expression profiling reveals the profound upregulation of hypoxia-responsive genes in primary human astrocytes. Physiol Genomics 2006;25:435–449. [PubMed: 16507782]

Michailov GV, Sereda MW, Brinkmann BG, Fischer TM, Haug B, Birchmeier C, Role L, Lai C, Schwab MH, Nave KA. Axonal neuregulin-1 regulates myelin sheath thickness. Science 2004;304:700–703. [PubMed: 15044753]

Mimmack ML, Ryan M, Baba H, Navarro-Ruiz J, Iritani S, Faull RL, McKenna PJ, Jones PB, Arai H, Starkey M, et al. Gene expression analysis in schizophrenia: reproducible up-regulation of several members of the apolipoprotein L family located in a high-susceptibility locus for schizophrenia on chromosome 22. Proc Natl Acad Sci U S A 2002;99:4680–4685. [PubMed: 11930015]

Nedergaard M, Dirnagl U. Role of glial cells in cerebral ischemia. Glia 2005;50:281–286. [PubMed: 15846807]

Newland MC. Animal models of manganese's neurotoxicity. Neurotoxicology 1999;20:415–432. [PubMed: 10385901]

Newman EA. New roles for astrocytes: regulation of synaptic transmission. Trends Neurosci 2003;26:536–542. [PubMed: 14522146]

Pal PK, Samii A, Calne DB. Manganese neurotoxicity: a review of clinical features, imaging and pathology. Neurotoxicology 1999;20:227–238. [PubMed: 10385886]

Park JY, Su YQ, Ariga M, Law E, Jin SL, Conti M. EGF-like growth factors as mediators of LH action in the ovulatory follicle. Science 2004;303:682–684. [PubMed: 14726596]

Parslow, TG.; Stites, DP.; Terr, AI.; Imboden, JB. Medical Immunology. New York: Lange Medical Books; 2001.

Plafker SM, Macara IG. Importin-11, a nuclear import receptor for the ubiquitin-conjugating enzyme, UbcM2. Embo J 2000;19:5502–5513. [PubMed: 11032817]

Robinson JK. Galanin and cognition. Behav Cogn Neurosci Rev 2004;3:222–242. [PubMed: 15812108]

Schlessinger J. Common and distinct elements in cellular signaling via EGF and FGF receptors. Science 2004;306:1506–1507. [PubMed: 15567848]

Schroder K, Hertzog PJ, Ravasi T, Hume DA. Interferon-gamma: an overview of signals, mechanisms and functions. J Leukoc Biol 2004;75:163–189. [PubMed: 14525967]

Suzuki Y, Mouri T, Nishiyama K, Fujii N. Study of subacute toxicity of manganese dioxide in monkeys. Tokushima J Exp Med 1975;22:5–10. [PubMed: 821178]

Tait CR, Jones PF. Angiopoietins in tumours: the angiogenic switch. J Pathol 2004;204:1–10. [PubMed: 15307132]

Wang Z, Trillo-Pazos G, Kim SY, Canki M, Morgello S, Sharer LR, Gelbard HA, Su ZZ, Kang DC, Brooks AI, et al. Effects of human immunodeficiency virus type 1 on astrocyte gene expression and function: potential role in neuropathogenesis. J Neurovirol 2004;10:25–32. [PubMed: 14982736]

Wasserman, GA.; Liu, X.; Parvez, F.; Ahsan, H.; Levy, D.; Factor-Litvak, P.; Kline, J.; van Geen, A.; Slavkovich, V.; LoIacono, NJ., et al. Environ Health Perspect. 2005. Water Manganese Exposure and Children's Intellectual Function in Araihazar, Bangladesh. in press

Wrenn CC, Kinney JW, Marriott LK, Holmes A, Harris AP, Saavedra MC, Starosta G, Innerfield CE, Jacoby AS, Shine J, et al. Learning and memory performance in mice lacking the GAL-R1 subtype of galanin receptor. Eur J Neurosci 2004;19:1384–1396. [PubMed: 15016096]

Glossary

ANOVA
: analysis of variance

Mn
: manganese

IFN-γ
: interferon gamma

EGF
: epidermal growth factor

VEGF
: vascular endothelial growth factor

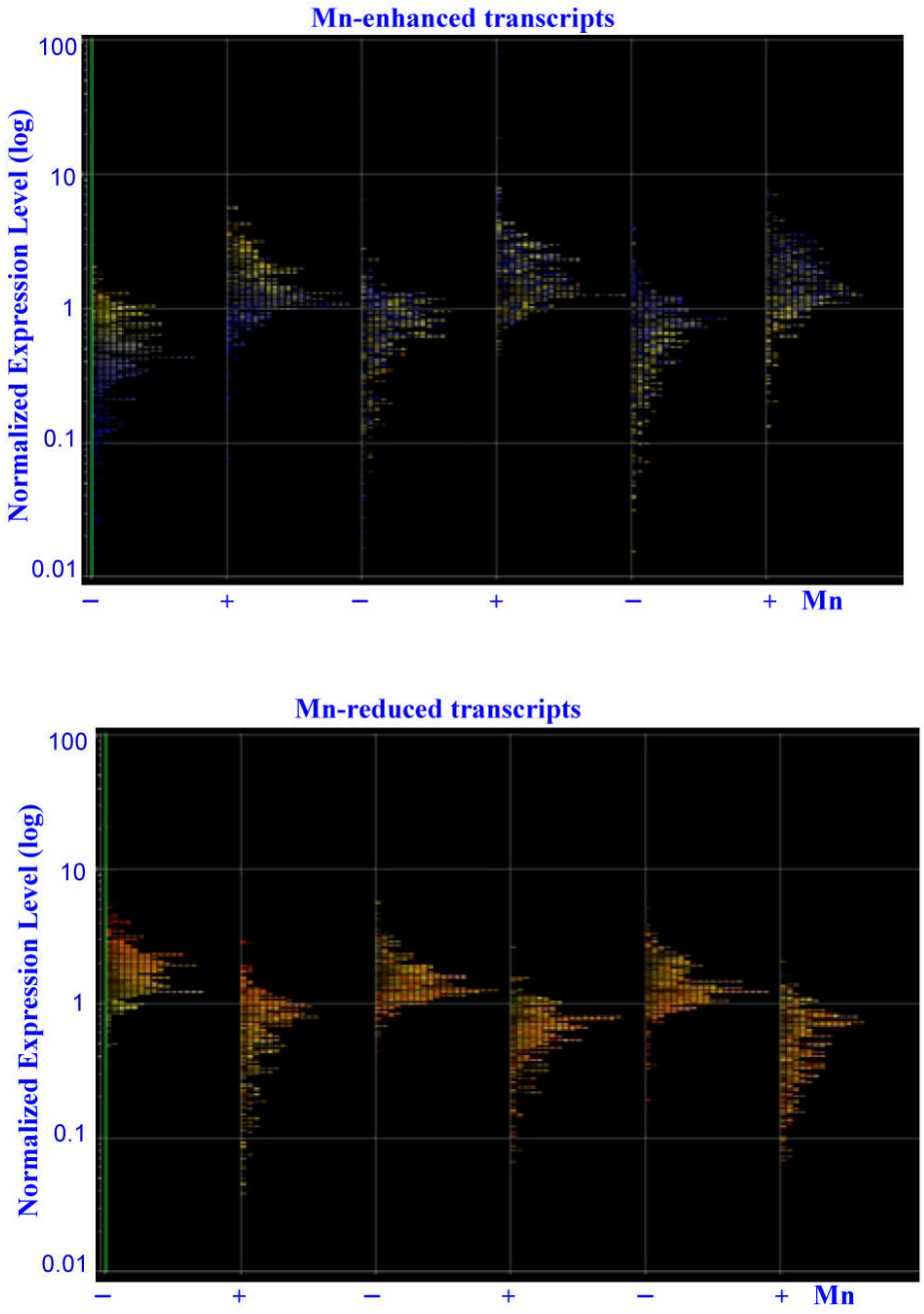

Figure 1.

Graphic illustration of the normalized expression levels of Mn^{2+}-altered genes in primary human astrocytes. Primary human astrocytes were treated with or without 200 μM Mn^{2+} for 7 days. RNA samples were extracted from these cells, and cRNA probes were generated and were hybridized to the Human Genome U133 Plus 2.0 arrays and scanned. Data were analyzed by using various algorithms in GeneSpring, including nonparametric two-way ANOVA, and with the Benjamini & Hochberg false discovery rate multiple testing correction (p-value less than 0.05). The differentially expressed genes in Mn^{2+}-treated vs. untreated cells were subjected to four consecutive filtering processes to identify genes whose overall expression level in three independent batches of astrocytes was altered at least twofold and whose

expression level in each batch of astrocytes was altered at least 1.5-fold. The expression levels of up-regulated genes (Top) and down-regulated genes (Bottom) by Mn^{2+} in three batches of independent astrocytes were plotted.

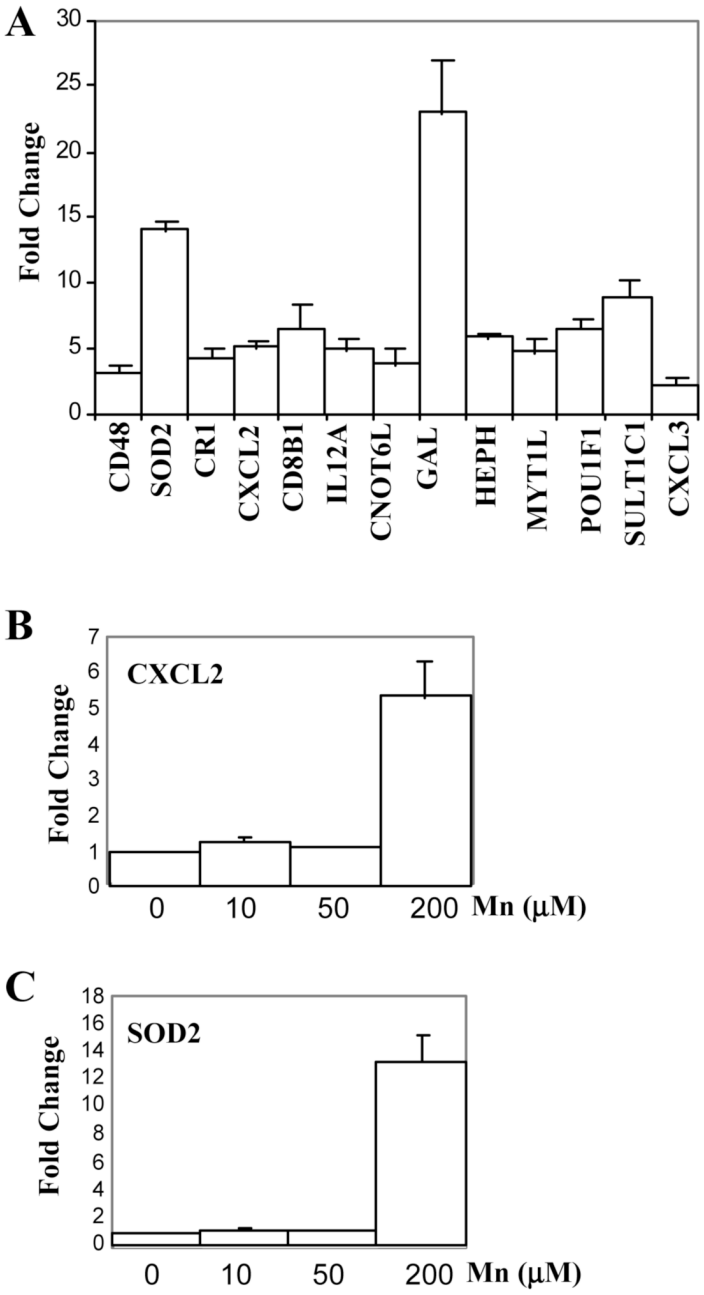

Figure 2.

(A) Real-time RT-PCR analysis of the induction of the transcript levels of genes induced by Mn^{2+} in primary human astrocytes. Total RNA from three to six independent batches of human astrocytes was isolated, and real-time RT-PCR analysis was performed as described in Materials and Methods. β-actin was used as an internal standard. The folds of induction of the indicated transcript levels were calculated by using Roche software, as described in Materials and Methods. Abbreviations: CD48, CD48 antigen (B-cell membrane protein); SOD2, superoxide dismutase 2; CR1, complement component receptor 1; CXCL2, chemokine (C-X-C motif) ligand 2; CD8B1, CD8 antigen, beta polypeptide; IL12A, interleukin 12A; CNOT6L, CCR4-NOT transcription complex, subunit 6-like; GAL, galanin; HEPH, hephaestin; MYT1L,

myelin transcription factor 1-like; POU1F1, POU domain, class 1, transcription factor 1; SULT1C1, sulfotransferase family, cytosolic, 1C, member; and CXCL3, chemokine (C-X-C motif) ligand 3. (B) Real-time RT-PCR analysis of the CXCL2 transcript level at different $MnCl_2$ concentrations. Total RNA was isolated from human astrocytes treated with 0, 10, 50, or 200 μM $MnCl_2$ for 7 days, and real-time RT-PCR analysis of CXCL2 transcript was performed as in A. (C) Real-time RT-PCR analysis of the SOD2 transcript level at different $MnCl_2$ concentrations. Total RNA was isolated from human astrocytes treated with 0, 10, 50, or 200 μM $MnCl_2$ for 7 days, and real-time RT-PCR analysis was performed as in A.

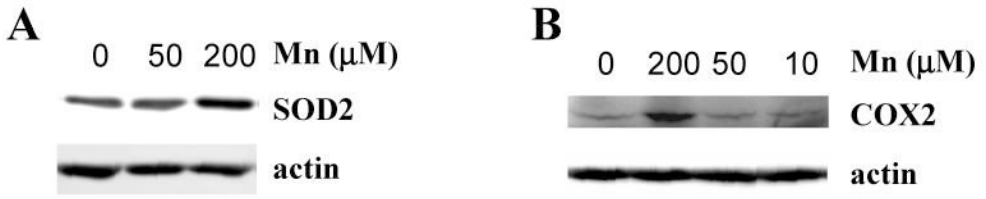

Figure 3.

The effect of $MnCl_2$ on the protein levels of SOD2 (A) and COX2 (B). Human astrocytes were treated with 0, 10, 50, or 200 μM $MnCl_2$ for 7 days. Then protein extracts were prepared and subjected to Western blotting analysis. The PVDF membranes were probed with antibodies against SOD2, COX2 and β-actin, respectively. Equal amounts of cellular proteins were loaded in every lane.

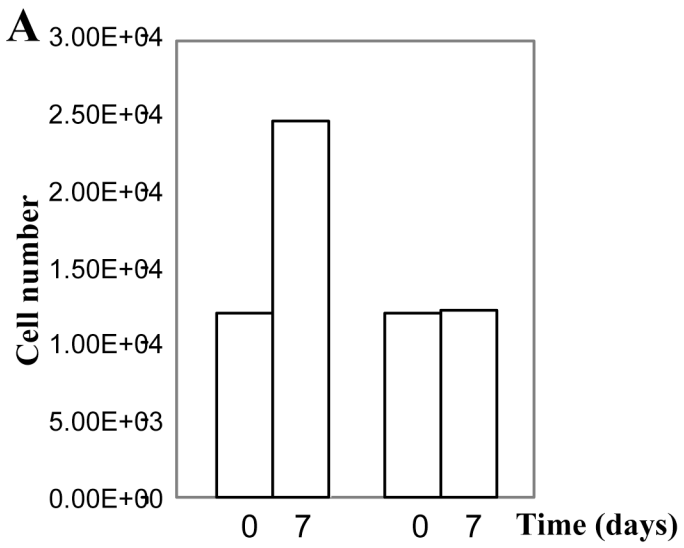

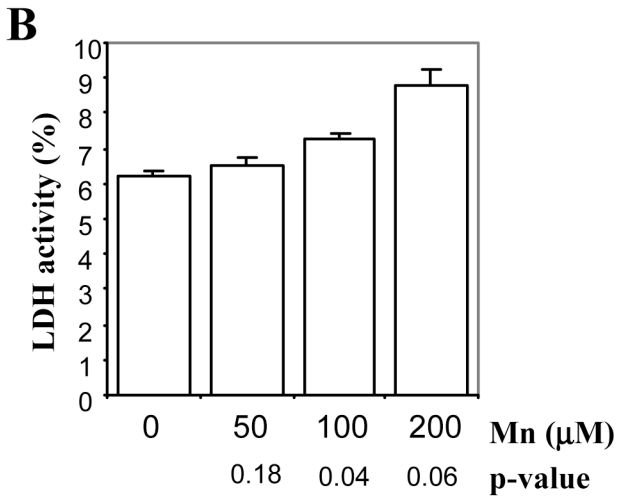

Figure 4.

(A) The effect of $MnCl_2$ on the growth of primary human astrocytes. Human astrocytes were treated with 0 or 200 μM $MnCl_2$ for 7 days. Then, cells were counted as described in Materials and Methods. The data plotted here were calculated from six independent experiments. The error bars are plotted, but are too small to be discernable. (B) The effect of $MnCl_2$ on LDH release by primary human astrocytes. Human astrocytes were treated with 0, 10, 50, or 200 μM $MnCl_2$ for 7 days. Then, LDH released to medium was measured and calculated as percentage of total cellular LDH activity, as described in Materials and Methods. The data plotted here were calculated from six independent experiments. Two-tailed t-tests were performed to compare $MnCl_2$-treated cells with untreated cells. P values were calculated by using the SAS software.

Table 1

Numbers of Transcripts Altered by Mn in Primary Human Astrocytes*

Tot (annotated)	Cyto	Cell	Transp	Dev	Sign Trans	Trans Reg
734(316) < 414+ 320−	30 < 28+ 2−	15 −	36 < 18+ 18−	38 < 25+ 13−	41 < 26+ 15−	30 < 13+ 17−

*The up-regulated and down-regulated genes in primary human astrocytes (Figure 1) were categorized by using the NIH DAVID annotation program and the Gene Ontology algorithm in GeneSpring. Listed here are the numbers of altered genes encoding cytokine and inflammatory functions (Cyto), regulators of cell cycle and DNA replication and repair (Cell), transporters (Transp), transcriptional regulators (Trans Reg) and signal transducers (Sign Trans), and those with developmental-relevant functions (Dev). The total (Tot) number of altered transcripts by Mn is also shown; the number of annotated(classified) genes is shown in parentheses. “+” indicates upregulated genes while “–” indicates down-regulated genes.

Table 2

List of Mn-down-regulated Genes Controlling Cell Cycle and DNA Replication

Gene Name	Fold Change	Common	Genbank	Description
1553387_at	0.5	ATM	NM_138293	ataxia telangiectasia mutated
209642_at	0.5	BUB1	AF043294	BUB1 budding uninhibited by benzimidazoles 1 homolog
204238_s_at	0.5	C6orf108	NM_006443	chromosome 6 ORF 108
202705_at	0.4	CCNB2	NM_004701	cyclin B2
204159_at	0.3	CDKN2C	NM_001262	cyclin-dependent kinase inhibitor 2C
1555758_a_at	0.5	CDKN3	AF213040	cyclin-dependent kinase inhibitor 3
204170_s_at	0.5	CKS2	NM_001827	CDC28 protein kinase regulatory subunit 2
218689_at	0.4	FANCF	NM_022725	Fanconi anemia, complementation group F
201539_s_at	0.4	FHL1	U29538	four and a half LIM domains 1
201755_at	0.3	MCM5	NM_006739	MCM5 minichromosome maintenance deficient 5
211450_s_at	0.5	MSH6	D89646	mutS homolog 6
205053_at	0.3	PRIM1	NM_000946	nascent-polypeptide-associated complex alpha polypeptide
205628_at	0.4	PRIM2A	NM_000947	primase, polypeptide 2A
203209_at	0.5	RFC5	BC001866	replication factor C
206067_s_at	0.3	WT1	NM_024426	Wilms tumor 1

Table 3

The effect of Mn on cell cycle progression*

	Control	Mn-treated	p-value
G1	$55.8^{\pm 0.9}$	$36.7^{\pm 1.3}$	0.0003
S	$36.3^{\pm 1.1}$	$54.9^{\pm 1.3}$	0.0003
G2	$3.8^{\pm 0.7}$	$4.5^{\pm 0.2}$	0.57

* Primary human astrocytes treated with no reagent (control) or 200 μM $MnCl_2$ (Mn-treated) for 7 days were subjected to flow cytometric analysis as described in Materials and Methods. The shown data are averages from three experiments, and the two-tailed t-test p-value was calculated by using the SAS software.

Table 4

List of Mn-up-regulated Genes Encoding Cytokine and Inflammatory Functions

Gene Name	Fold Change	Common	Genbank	Description
202912_at	3.8	ADM	NM_001124	adrenomedullin
221009_s_at	10	ANGPTL4	NM_016109	angiopoietin-like 4
223333_s_at			AF169312	
208075_s_at	3.1	CCL7	NM_006273	chemokine (C-C motif) ligand 7
233137_at	4.2	CD48	AF143887	CD48 antigen
1553562_at	5.1	CD8B1	NM_172100	CD8 antigen, beta polypeptide 1 (p37)
208488_s_at	4.2	CR1	NM_000651	complement component (3b/4b) receptor 1
237038_at	2.4	CXCL14	AI927990	chemokine (C-X-C motif) ligand 14
218002_s_at			NM_004887	
222484_s_at			AF144103	
209774_x_at	4.1	CXCL2	M57731	chemokine (C-X-C motif) ligand 2
204470_at			NM_001511	
207850_at	4.7	CXCL3	NM_002090	chemokine (C-X-C motif) ligand 3
206336_at	2.4	CXCL6	NM_002993	chemokine (C-X-C motif) ligand 6
224239_at	3.2	DEFB103	AF301470	defensin, beta 103
203717_at	2.8	DPP4	NM_001935	dipeptidylpeptidase 4
205767_at	8.8	EREG	NM_001432	epiregulin
221577_x_at	2.7	GDF15	AF003934	growth differentiation factor 15
209728_at	3.5	HLA-DRB4	BC005312	major histocompatibility complex, class II, DR beta 3
207160_at	4.2	IL12A	NM_000882	interleukin 12A
206693_at	2.5	IL7	NM_000880	interleukin 7
1554544_a_at	2.4	MBP	L18865	CDNA clone MGC:70813
206560_s_at	3.6	MIA	NM_006533	melanoma inhibitory activity
209652_s_at	2.9	PGF	BC001422	placental growth factor
204748_at	2.7	PTGS2	NM_000963	prostaglandin-endoperoxide synthase 2
206157_at	2.3	PTX3	NM_002852	pentaxin-related gene
212171_x_at	2.0	VEGF	H95344	vascular endothelial growth factor
211527_x_at			M27281	

Table 5

List of Genes That Were Affected Similarly by Mn^{2+} and Hypoxia

Gene Name	Fold Change	Common	Genbank	Description
216113_at	4.3	ABI2	AF070566	abl interactor 2
202912_at	3.8	ADM	NM_001124	adrenomedullin
223333_s_at	11	ANGPTL4	AF169312	angiopoietin-like 4
221009_s_at	8.8	ANGPTL4	NM_016109	angiopoietin-like 4
205678_at	2.2	AP3B2	NM_004644	adaptor-related protein complex 3, beta 2 subunit
213606_s_at	0.5	ARHGDIA	AI571798	Rho GDP dissociation inhibitor (GDI) alpha
205109_s_at	2.4	ARHGEF4	NM_015320	Rho guanine nucleotide exchange factor (GEF) 4
243062_at	6.9	BHD	AV694665	folliculin
1553202_at	0.2	C10orf24	NM_152709	chromosome 10 ORF 24
232635_at	0.4	C14orf145	AV703868	chromosome 14 ORF 145
235616_at	3.2	C20orf17	AI694059	chromosome 20 ORF 17
218541_s_at	2.6	C8orf4	NM_020130	chromosome 8 ORF 4
228302_x_at	2.5	CaMKIINalpha	AW162846	CAM-KII INHIBITORY PROTEIN
1554411_at	0.3	CTNNB1	AB062292	catenin, beta 1, 88kDa
208282_x_at	0.1	DAZ2	NM_020363	deleted in azoospermia 2
1570227_at	2.8	DKFZP434K046	BC016065	hypothetical protein
239380_at	17	FIS	AI190413	Homo sapiens cDNA clone
219650_at	0.4	FLJ20105	NM_017669	
238949_at	2.1	FLJ31951	BF681162	Homo sapiens cDNA clone
1559652_at	0.3	FLJ35954	BM722867	Homo sapiens cDNA clone
227902_at	4.4	FLJ38705	AK024438	hypothetical protein
1554154_at	4.6	GDAP2	BC013132	ganglioside induced differentiation associated protein 2
230498_at	3.8	GPR24	AI934819	G protein-coupled receptor 24
216417_x_at	0.3	HOXB9	X16172	Human HOX-2.5
207160_at	4.2	IL12A	NM_000882	interleukin 12A
206693_at	2.5	IL7	NM_000880	interleukin 7
229261_at	2.1	ITGA3	BF508819	integrin, alpha 3
221841_s_at	3.2	KLF4	BF514079	Kruppel-like factor 4 (gut)
227868_at	2.3	LOC154761	AI928764	Homo sapiens cDNA clone
227016_at	2.6	LOC157697	AA767385	hypothetical protein
222336_at	3.0	LOC201895	AW974915	hypothetical protein
222037_at	0.2	MCM4	AI859865	Homo sapiens cDNA clone
201755_at	0.3	MCM5	NM_006739	minichromosome maintenance deficient 5
1554540_at	0.2	MGC27277	BC042869	hypothetical protein
238560_at	2.7	NDP52	AI684710	nuclear domain 10 protein
206686_at	3.6	PDK1	NM_002610	pyruvate dehydrogenase kinase 1
226452_at	3.2	PDK1	AU146532	pyruvate dehydrogenase kinas 1
217705_at	2.6	PRKCM	AW085172	protein kinase C, mu
206157_at	2.3	PTX3	NM_002852	pentaxin-related gene
214409_at	3.4	RFPL3S	AL021937	
217691_x_at	2.2	SLC16A3	AA853175	monocarboxylic acid transporter 3
215078_at	12	SOD2	AL050388	superoxide dismutase 2
243834_at	3.0	TNRC6	BF507964	trinucleotide repeat containing 6
205694_at	0.3	TYRP1	NM_000550	tyrosinase-related protein 1
231990_at	0.2	USP15	AK023703	ubiquitin specific protease 15
211527_x_at	2.0	VEGF	M27281	vascular endothelial growth factor
212171_x_at	2.0	VEGF	H95344	vascular endothelial growth factor
206067_s_at	0.3	WT1	NM_024426	Wilms tumor 1
232427_at	3.1	ZNF224	BE464105	zinc finger protein 224
233944_at	4.8		AU147118	CDNA FLJ12079 fis
234021_at	3.9		AK024984	CDNA: FLJ21331 fis,
1558783_at	3.7		AK024805	CDNA: FLJ21152 fis
1559760_at	3.6		BC036933	

Gene Name	Fold Change	Common	Genbank	Description
244175_at	3.5		BF223582	cDNA clone
1559053_at	3.4		BC027905	cDNA clone
239567_at	3.2		AW974998	CDNA clone
1565913_at	2.5		H59257	cDNA clone
1558447_at	2.4		BC032415	CDNA clone
232876_at	2.3		AK025534	cDNA clone
213931_at	2.3		AI819238	repressor Id-2 - human
213003_s_at	2.2		BF061054	CEBP DELTA
240094_at	2.2		AL042660	Transcribed sequences
235242_at	2.1		BE739287	Homo sapiens cDNA clone I
1562529_s_at	2.0		BC040965	cDNA clone
234957_at	0.5		AF017336	
220859_at	0.5		NM_014136	
223661_at	0.4		AF130080	CDNA clone
231223_at	0.2		R41565	Transcribed sequences

Table 6

List of Mn-altered Genes That Are Regulated by the IFN-γ or EGF Signaling Pathway

Gene Name	Fold Change	Common	Genbank	Description
	IFNγ-regulated			
202912_at	3.8	*ADM*[*]	NM_001124	adrenomedullin
208644_at	0.5	ADPRT	M32721	ADP-ribosyltransferase
202095_s_at	0.4	BIRC5	NM_001168	baculoviral IAP repeat-containing 5
208075_s_at	3.1	*CCL7*	NM_006273	chemokine (C-C motif) ligand 7
233137_at	4.2	*CD48*	AF143887	CD48 antigen (B-cell membrane protein)
213003_s_at	2.3	*CEBPD*	BF061054	CCAAT/ENHANCER BINDING PROTEIN DELTA
209774_x_at	4.1	*CXCL2*	M57731	chemokine (C-X-C motif) ligand 2
204470_at			NM_001511	
224239_at	3.2	*DEFB103*	AF301470	defensin, beta 103
203717_at	2.8	*DPP4*	NM_001935	dipeptidylpeptidase 4
207160_at	4.2	*IL12A*	NM_000882	interleukin 12A
215182_x_at	2.5	*IL1R1*	AL050122	
221841_s_at	3.2	*KLF4*	BF514079	Kruppel-like factor 4 (gut)
240338_at	2.2	*LRAP*	AI807341	leukocyte-derived arginine aminopeptidase
244704_at	0.5	NFYB	AW083948	neuronal thread protein
200790_at	0.4	ODC1	NM_002539	ornithine decarboxylase 1
1559400_s_at	5.4	PAPPA	BG620958	
211840_s_at	0.4	PDE4D	U50157	phosphodiesterase 4D, cAMP-specific
204748_at	2.7	*PTGS2*	NM_000963	prostaglandin-endoperoxide synthase 2
203110_at	0.4	PTK2B	U43522	PTK2B protein tyrosine kinase 2 beta
206157_at	2.3	PTX3	NM_002852	pentaxin-related gene, rapidly induced by IL-1 beta
228037_at	0.4	RARA	AA404273	retinoic acid receptor, alpha
1568765_at	2.3	SERPINE1	BC020765	serine (or cysteine) proteinase inhibitor, clade E, member 1
237106_at	2.2	*SLC11A2*	AI051244	solute carrier family 11, member 2
215078_at	12	*SOD2*	AL050388	superoxide dismutase 2
212171_x_at	2.0	*VEGF*	H95344	vascular endothelial growth factor
211527_x_at			M27281	
	EGF-regulated			
221681_s_at	2.0	DSPP	AF094508	Homo sapiens dentin phosphoryn mRNA, complete cds.
236990_at	0.2	EIF2AK3	AV699382	cDNA clone
205767_at	8.7	EREG	NM_001432	epiregulin
234240_at	0.2	GSN	AL049930	Homo sapiens mRNA
209957_s_at	0.4	NPPA	M30262	natriuretic peptide precursor A
233626_at	4.3	NRP1	AK024580	neuropilin 1
202730_s_at	0.4	PDCD4	NM_014456	programmed cell death 4
205934_at	0.4	PLCL1	NM_006226	phospholipase C-like 1
217705_at	2.6	PRKCM	AW085172	protein kinase C, mu
202388_at	2.1	RGS2	NM_002923	regulator of G-protein signalling 2
220983_s_at	2.1	SPRY4	NM_030964	sprouty homolog 4

[*] The italicized genes are those known to be activated by INF-γ and were up-regulated by Mn